ISSN (Print) 1226-1750
ISSN (Online) 2233-6656
Journal of Magnetics 22(4), 654-661 (2017) https://doi.org/10.4283/JMAG.2017.22.4.654

Analysis of the Brain-activation Areas During the Visual Stimulations of 2D and 3D Imagery using Functional Magnetic Resonance Imaging

Yeong-Cheol Heo[1], Hae-Kag Lee[2], and Jae-Hwan Cho[3]*

[1]*Department of Radiologic Science, College of Health sciences EulJi University, Seongnam 13135, Republic of Korea*
[2]*Department of Computer Science and Engineering, Soonchunhyang University, Asan 31538, Republic of Korea*
[3]*Department of Radiological Technology, Ansan University, Asan 15518, Republic of Korea*

(Received 16 October 2017, Received in final form 4 December 2017, Accepted 4 December 2017)

The aim of this study is an functional magnetic resonance imaging (fMRI) investigation of the activity of the Brodmann brain areas during the viewing of 2D and 3D images. By using the 3.0 Tesla MRI system, an 8-channel SENSE Head Coil, and the ESys fMRI system in 5 adult males, 3D T1-weighted images were obtained from anatomic images. A gradient-EPI sequence was used for the acquisition of the brain functional images. The monitor was installed so that the images could be seen through a mirror located in the coil. The 3D appearance of the triangular, cubic, and hexagonal shapes were visually stimulated by the 2D and 3D images, and a pair of red–blue cardboard glasses was worn during the viewing of the 3D images. The display object is composed of 4 stimulus projections every 60 s and 4 resting periods of 20 s every 20 s. The acquired data were analyzed using the SPM-8 program. For the 2D imagery, the activation area of the brain is larger than that of the 3D imagery ($p < .05$). In the visual-cortex activation area, the number of clusters is larger for the 3D imagery ($p < .05$). It is expected that the basic data of this study will be used to analyze the effects of 3D-image contents on the areas of the human brain.

Keywords : functional magnetic resonance imaging, visual cortex, brodmann area, 3D visual fMRI, visual stimulation

1. Introduction

Modern people are obtaining approximately 80 % of their information through various display devices such as computers, smart phones, and televisions [1]. Display technology is now presented in both two-dimensional (2D) and three-dimensional (3D) forms, but the prediction that 3D display technology will lead the future of the industry can be made fairly confidently. The considerable change that was introduced by 3D video pioneered a new genre in the display industry, such as the previous transitions from silent film to oily film and from black-and-white TV to color TV. Especially in the movie industry, the use of 3D technology has been steadily growing since the production of the movie Avatar [2]. The viewing images of 3D technology reflect the human desire for realistic images and new brain experiences [3]. However, a number of particular inconveniences affect many people who have seen 3D displays compared with 2D displays, and accordingly, a number of studies have been completed. Based on a questionnaire survey of 953 subjects, Solimini *et al.* [4] reported that the headache was experienced by 13.7% of those who viewed 3D movies, and this occurred immediately in 16.8 % of the subjects, while 8.3% of the subjects were affected at the 2-hr time point. Read and Bohr [5] reported on 433 3D viewers in a postsubjective evaluation, where 14 % of the participants reported eyestrain and headache complaints. In addition, Taylor *et al.* [6] reported a case wherein a 55-year-old woman experienced symptoms of Takotsubo cardiomyopathy with extreme palpitations, nausea, vomiting, and malaise for 48 hr after watching a 3D action movie. Taken together, these reports show that 3D imaging stimulates the human brain and causes side-effects in various forms; therefore, a medical interpretation of the nature of the stimulation that 3D imagery is exerting on the human brain is needed. Functional magnetic resonance imaging (fMRI) is a state-of-the-art technique that stimulates specific brain regions and signals and analyzes the corresponding brain-cortex sites in response to changes

*Corresponding author: Tel: +82-31-363-7703
Fax: +82-31-400-6941, e-mail: 8452404@hanmail.net

in the blood-oxygen dependence. Therefore, in this study, basic fMRI research data on the effect of 3D imagery on the brain was provided through the activation-level differences of the brain cortex during the viewing of 2D and 3D images.

2. Subjects and Methods

Five medically healthy men (mean age 33.6 ± 2.7 years) were included. The test equipment are the Achieva Release 2.5 3.0 Tesla magnetic resonance imaging (MRI) system (Philips Healthcare, U.S.A.) and the Achieva Release 2.5 8-Channel SENSE Head Coil (Philips Healthcare, U.S.A.). A reflector was attached to the coil so that the visual-stimulus image could be seen through the reflector. The instrument that was used for the visual stimulation is the ESys fMRI Manager Client (Invivo, U.S.A.), and a pair of red–blue cardboard glasses (BOS, Republic of Korea) was used for the 3D-image visual stimulation (Fig. 1). The blood-oxygen level-dependent (BOLD) effect of the fMRI can be explained using a very simple equation [7]. From the MRI signal, the magnetic-resonance (MR) signal is exponentially dependent on the echo time (TE) value, and therefore the following equation is used:

$$S = S_0 \cdot e^{-TE \cdot R_2^*} \tag{1}$$

where S_0 will be measurable if the TE can be reduced to zero with an effective spin density.

$$R_2^* = R_0 + R \tag{2}$$

In Equation (2), if deoxyhemoglobin does not exist, then the R is relaxed by additional deoxyhemoglobin and the R_0 becomes R_2^*. In general, the R_0 is much larger than the R, and the additional effect of the deoxyhemoglobin is negligible because T2*, where the signal is reduced, is mainly determined by T2 and a large field gradient through the voxel. Therefore, the relaxation constant of the transverse-relaxation rate R_2^* is recorded as the sum of the R_0 and the R. Assuming that the R is activated only by a parameter change, the activation is changed according to "rest" and "act"; therefore, the following equations apply:

$$\Delta S = S_{act} - S_{rest} \tag{3}$$

$$\frac{\Delta S}{S_{rest}} = e^{-\Delta R \cdot TE} - 1 \approx -\Delta R \cdot TE \tag{4}$$

$$\Delta R = R_{act} - R_{rest} \tag{5}$$

where the magnitude of the magnetic field ΔB near the magnetized blood veesel is equal to the value that is obtained from the multiplication of the main magnet by the blood and the peripheral blood-vessel space, and a proportional equation of $\Delta X \cdot \Delta B_0$ is consequently established. The ΔX is linearly dependent on the local-deoxyhemoglobin concentration in the blood, which can be explained by the change in the oxygen-extraction fraction E. The deoxyhemoglobin-produced local-field offset is changed as follows:

$$\Delta B \propto B_0 \cdot E \tag{6}$$

However, in an irregular magnetic field, the spins are affected by different magnetic fields, and therefore the phase directions are different for each spin. That is, it is this phase dispersion that determines the R_2^* at the time of the data acquisition. Therefore, the uniformity of the magnetic field is required to prevent the diffusion of the phase dispersion, so the field-distortion magnitude between the R and the ΔB can be explained by the following exponential relationship:

$$R \propto \Delta B^{\beta} \tag{7}$$

where the β approaches 1 when the diffusion is not important, and when the diffusion is important, the β approaches 2. That is, the signal change that is due to the intravascular diffusion is $\beta \approx 2$, and $\beta \approx 1$ is appropriate in the regions where the effect of the deoxyhemoglobin is minor, like in the veins. So even if the oxygen concentration of the blood does not change and the venous blood flow (V) increases, the total deoxyhemoglobin increases, so that the R value is increased and the net magnetization

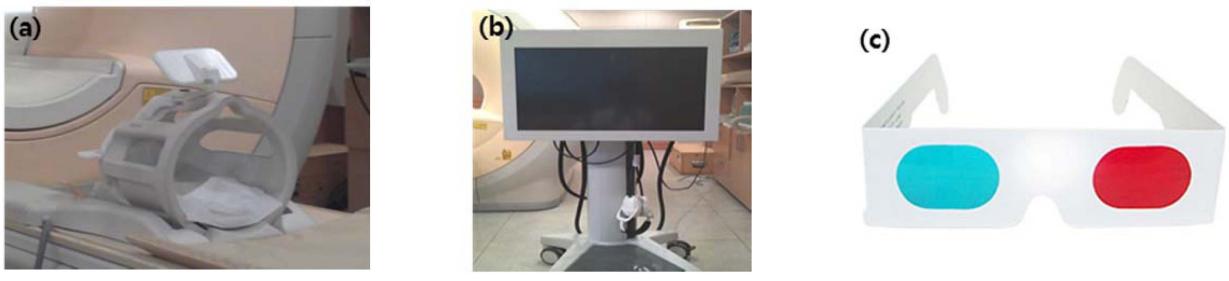

Fig. 1. (Color online) 8-Channel SENSE Head Coil (a), ESys fMRI Manager Client (b), and 3D Red-Blue Cardboard Glasses (c).

is decreased. Therefore, when it is assumed that the R is proportional to the V, it is possible to combine the previously mentioned factors and represent the BOLD signal as follows:

$$\frac{\Delta S}{S_{rest}} \approx TE \cdot k \cdot V_{act}[B_0 \cdot E_{act}]^{\beta} - k \cdot V_{rest} \cdot [B_0 \cdot E_{rest}]^{\beta} \quad (8)$$

$$= A \cdot \left[1 - \frac{V_{act}}{V_{rest}} \cdot \left(\frac{E_{act}}{E_{rest}}\right)^{\beta}\right] \quad (9)$$

where k is the net proportionality constant from all of the previously mentioned proportions, V is the blood volume, and A is the local scaling factor that is given by the following formula:

$$A = k \cdot TE \cdot V_{rest} \cdot [B_0 \cdot E_{rest}]^{\beta} \quad (10)$$

The BOLD-signal change is very simple because it depends on the change of the V value and the extraction-fraction E of the extractions of the water, the β, and the A [7]. For the experiment, the headphone that was attached to the equipment was placed on the ear of the subject, and the subject's head was laid flat on the 8-Channel SENSE Head Coil with a reflector to enable him to listen to the story from the outside. After the coils were placed in the center of the magnet bore so that they were suitable for inspection, it was confirmed whether the images that were displayed in the ESys fMRI Manager Client were visible. To obtain anatomic images, 3D T1-weighted images (repetition time [TR] = 8.2 ms, TE = 3.8 ms, recovery delay [TI] = 1026 ms, matrix = 240 × 236, slice number = 326, thickness = 0.5 mm, scan time = 4 min 35 s) were examined. The fMRI images were acquired using a GE-EPI (gradient echo-echo planar image) for which the following values are relevant: TR = 2000 ms, TE = 30 ms, matrix = 68 × 68, slice number = 28, thickness = 4.5 mm, scan dynamics = 160, and scan time = 5 min 32 s. To realize the 3D imagery, left and right images were displayed in red and blue on a black background and were viewed through the pair of red–blue glasses. In the red lens, only the black and red parts are visible, and in the blue lens, only the black and blue parts are displayed; therefore, the 3D stereoscopic effect could be felt by the participants. The task images that the visual stimuli showed are 2D and 3D images with the following three shapes: triangle, cube, and hexagon. The pair of red–blue glasses was removed for the first anatomical image and the 2D visual-stimulus image, but the pair of glasses was used for the 3D visual stimulation. The visual-stimulus method used a GE-EPI sequence with a total of four 60-s visual stimuli and four 20-s rests (Fig. 2). The data were analyzed using the Statistical Parametric Mapping (SPM) 8 program (University College London, U.K.). To minimize the errors in the signal changes that are due to the motion during the examination, a realignment was performed, and a coregistration was performed to achieve a match between the functional image and the anatomical 3D T1-weighted image. Then, the images that were obtained from the the Talairach coordinates were used to determine the active area of the brain and to confirm the number of clusters in that area. The number of clusters indicates the active areas of the brain. To compare the differences between the 2D and 3D visual-stimulus images, the difference between the two states was analyzed using a paired t-test, and $p < .05$ was considered as a statistically significant difference.

3. Results

In the 2D visual-stimulation results, the numbers of clusters are the highest in the Brodmann-Area (BA) 19,

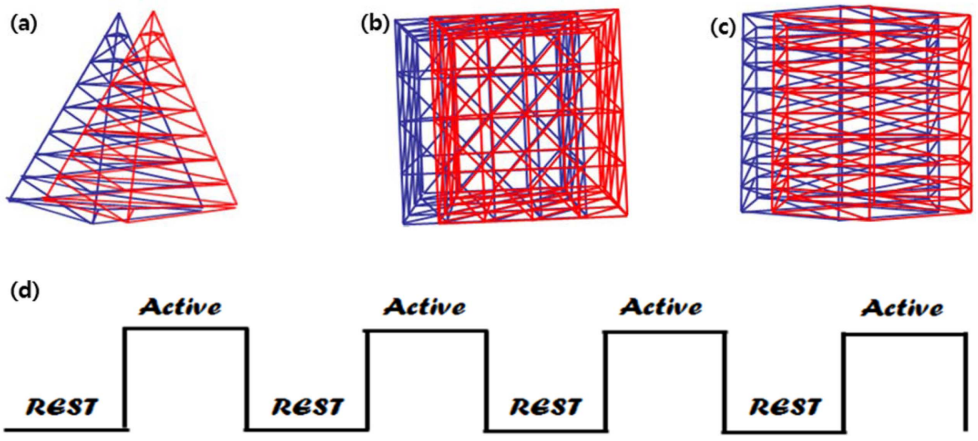

Fig. 2. (Color online) Three-Dimensional (3D) Visual-Stimulation Images: (a) triangular pyramid, (b) regular hexahedron or cube, (c) hexagonal prism, and (d) visual-stimulation design with 20 s of rest and 60 s of activity.

Table 1. Activation Areas During the Two-Dimensional (2D) Visual Stimulation.

Brain-Cortex Region			BA	Talairach coordinate			Z score	Cluster
				X	Y	Z		
Visual Stimuli of 2D > Fixation								
Right	**Frontal Lobe**	**Precentral Gyrus**	**6**	46.65	-7.19	38.62	4.74	**564**
	Frontal Lobe	Inferior Frontal Gyrus	10	39.94	49.2	0.61	3.32	5
	Limbic Lobe	**Parahippocampal Gyrus**	**19**	41.52	-40.59	-4.27	3.98	**368**
	Limbic Lobe	Anterior Cingulate	24	11.99	27.8	8.92	3.21	21
	Limbic Lobe	Cingulate Gyrus	31	5.88	-43.89	30.85	3	11
	Occipital Lobe	**Fusiform Gyrus**	**19**	28.54	-58.98	-8.03	6.94	**8124**
	Parietal Lobe	**Postcentral Gyrus**	**1**	52.08	-17.23	44.97	5.75	**564**
	Parietal Lobe	**Inferior Parietal Lobule**	**40**	39.14	-29.86	39.95	4.16	**564**
	Parietal Lobe	Postcentral Gyrus	7	22.08	-51.02	64.68	4.04	10
	Temporal Lobe	**SubGyral**	**37**	45.15	-50.28	-1.52	3.41	**368**
	Temporal Lobe	**Middle Temporal Gyrus**	**37**	46.9	-61.99	2.8	3.29	**368**
	Temporal Lobe	Superior Temporal Gyrus	22	61.9	-13.1	2.28	2.9	6
Left	Frontal Lobe	Medial Frontal Gyrus	10	-4.46	56.88	0.58	5.37	147
	Frontal Lobe	Medial Frontal Gyrus	10	-13.77	62	6.31	5.11	147
	Frontal Lobe	Medial Frontal Gyrus	10	-4.51	61.95	6.47	4.63	147
	Frontal Lobe	Superior Frontal Gyrus	10	0.79	61.87	26.37	4.2	194
	Frontal Lobe	Superior Frontal Gyrus	8	-29.11	41.65	41.96	4.15	194
	Frontal Lobe	Superior Frontal Gyrus	10	-8.47	61.92	26.22	3.63	194
	Frontal Lobe	Superior Frontal Gyrus	6	-22.15	5.46	65.68	3.61	43
	Frontal Lobe	Middle Frontal Gyrus	6	-27.61	6.18	58.45	2.99	43
	Frontal Lobe	Inferior Frontal Gyrus	47	-35.92	29.62	-7.94	3.05	17
	Frontal Lobe	Superior Frontal Gyrus	8	-12.43	49.01	42.94	2.81	21
	Frontal Lobe	Middle Frontal Gyrus	6	-38.65	10.32	55.05	2.8	5
	Frontal Lobe	Superior Frontal Gyrus	10	-38.04	49.55	19.14	2.78	8
	Occipital Lobe	**Lingual Gyrus**	**17**	-12.45	-91.84	2.57	5.83	**8124**
	Parietal Lobe	Postcentral Gyrus	2	-47.89	-27.89	42.26	3.74	24
	Parietal Lobe	Postcentral Gyrus	40	-46.14	-30.46	49.26	3.06	24
	Sub-lobar	Insula	13	-38.34	-12.98	24.02	3.08	5
	Temporal Lobe	Superior Temporal Gyrus	22	-43.63	-25.59	-0.69	4.96	166
	Temporal Lobe	Middle Temporal Gyrus	21	-64.01	-32.94	-1.73	3.08	166
	Temporal Lobe	Middle Temporal Gyrus	21	-54.73	-32.81	-3.36	3	166
	Temporal Lobe	Superior Temporal Gyrus	21	-60.19	-6.53	-2.76	4.14	40

which is the fusiform-gyrus region of the right occipital lobe, and the BA 17, which is the lingual-gyrus region of the left occipital lobe. The 2D visual-stimulation results showed activity in various areas besides the visual cortex. Also, high levels of activity were observed in the region of the precentral gyrus of the right frontal lobe (BA 6, Cluster 564), the parahippocampal gyrus of the right limbic lobe (BA 19, Cluster 358), the right parietal lobe (BA 37, Cluster 368), the posterior gyrus (BA 1, Cluster 564), the inferior parietal lobule (BA 40, Cluster 564), the subgyral of the right temporal lobe (BA 37, Cluster 368), and the middle temporal gyrus (BA 37, Cluster 368). The highest activity levels in the 3D visual-stimulation results are in the lingual gyrus (BA 18, Cluster 6665) and in the middle occipital gyrus (BA 18, Cluster 6665) of the right occipital lobe, thereby influencing the visual cortex (Table 2). The results of the 3D visual stimulation showed a high activity not only in the visual cortex but also in the superior frontal gyrus (BA 6, Cluster 532), the medial frontal gyrus (BA 8, Cluster 532), and the superior frontal gyrus (BA 8, Cluster 532), as shown in Fig. 3. The 2D and 3D visual stimulations showed that the numbers of clusters for the main brain area are higher in the BA 17 (right cuneus of the occipital lobe and the lingual gyrus) and the BA 18 (right lingual gyrus of the occipital lobe and the left lingual gyrus), where $p < .05$. However, the postcentral gyrus of the right parietal lobe (BA 1), the precentral gyrus (BA 6), and the left-middle occipital

Table 2. Activation Areas During the Three-Dimensional (3D) Visual Stimulation.

	Brain-Cortex Region		BA	Talairach coordinate			Z score	Cluster
				X	Y	Z		
Visual Stimuli of 3D > Fixation								
Right	Frontal Lobe	Superior Frontal Gyrus	9	8.14	52.34	27.39	2.96	41
	Frontal Lobe	Superior Frontal Gyrus	9	4.44	63.36	30.17	2.83	8
	Limbic Lobe	Anterior Cingulate	24	6.52	24.8	1.33	3.23	9
	Occipital Lobe	**Lingual Gyrus**	**18**	**11.87**	**-90.05**	**-16.67**	**6.86**	**6665**
	Occipital Lobe	**Middle Occipital Gyrus**	**18**	**24.62**	**-89.82**	**-0.21**	**6.54**	**6665**
Left	Frontal Lobe	Medial Frontal Gyrus	10	-8.27	67.04	12.29	4.67	272
	Frontal Lobe	Superior Frontal Gyrus	10	-19.51	67.91	22.99	3.58	272
	Frontal Lobe	**Superior Frontal Gyrus**	**6**	**-7.15**	**26.92**	**57.15**	**3.76**	**532**
	Frontal Lobe	**Medial Frontal Gyrus**	**8**	**-10.63**	**30.37**	**41.21**	**3.68**	**532**
	Frontal Lobe	**Superior Frontal Gyrus**	**8**	**-12.57**	**31.55**	**48.49**	**3.58**	**532**
	Frontal Lobe	Middle Frontal Gyrus	8	-45.9	16.99	44.75	3.59	217
	Frontal Lobe	Inferior Frontal Gyrus	9	-47.65	3.14	32.6	3.05	217
	Frontal Lobe	Inferior Frontal Gyrus	9	-40.17	5.49	27.54	2.85	217
	Limbic Lobe	Cingulate Gyrus	31	-3.28	-35.87	26.05	3.76	18
	Limbic Lobe	Anterior Cingulate	25	0.95	19.24	0.71	2.79	9
	Occipital Lobe	Cuneus	19	-16.46	-86.81	28.21	3.4	5
	Parietal Lobe	Supramarginal Gyrus	40	-47.87	-38.72	37.63	3.59	38
	Temporal Lobe	Middle Temporal Gyrus	39	-44.13	-76.82	23.28	3.35	27

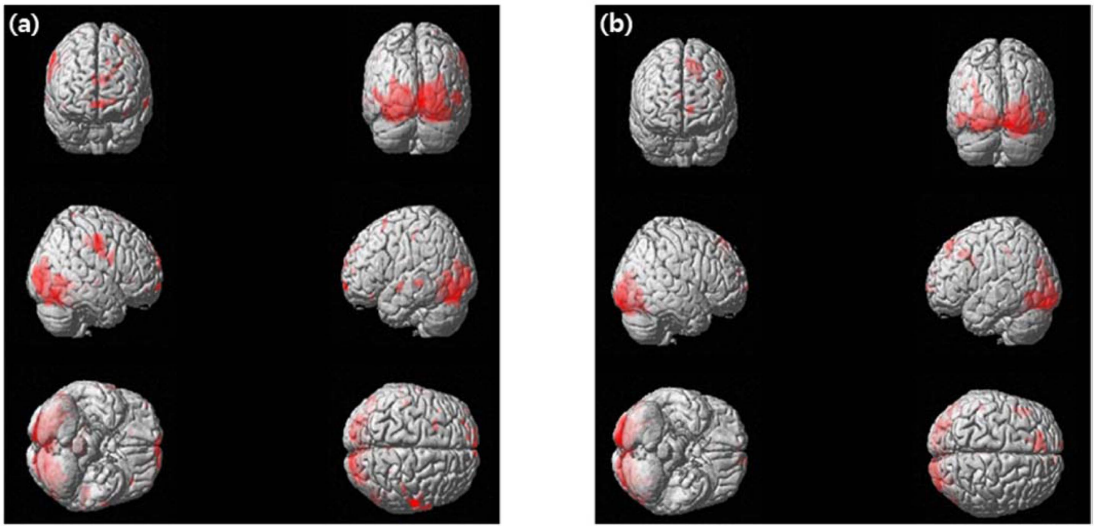

Fig. 3. (Color online) Activation Maps of Functional Magnetic Resonance Imaging (fMRI): (a) two-dimensional (2D) image and (b) three-dimensional (3D) image

gyrus (BA 37) showed a higher activity for the 2D visual stimulation ($p < .05$).

4. Discussion

Display technology is used in various fields such as those regarding computers, smartphones, televisions, cinema, and medicine. Display technology is developing in a way that its imagery is the best replication of reality that is presently available, and its 3D development originates in the black-and-white, color, and 2D technologies of the past. However, various medical symptoms such as eyestrain, headache, and Takotsubo cardiomyopathy have been reported after the viewing of 3D images [5, 6]. Until now, a lack of medical data on the causes of these symptoms has been an issue. The function of the brain is unique, and

Table 3. Results of Comparison between the Two-Dimensional (2D) and Three-Dimensional Visual Stimulations.

Brain-Cortex Region			BA	Talairach coordinate			Z score	Cluster	*p*
				X	Y	Z			
Visual Stimuli of 2D > 3D									
Right	Occipital Lobe	Cuneus	17	11.61	-90.1	3.14	4.27	89	< .05
	Occipital Lobe	Lingual Gyrus	18	15.42	-85.7	-3.58	4.1	89	
	Parietal Lobe	Postcentral Gyrus	3	29.74	-38	47.84	3.7	10	
	Parietal Lobe	Postcentral Gyrus	2	55.78	-19.11	44.55	2.8	14	
Left	Occipital Lobe	Lingual Gyrus	17	-10.58	-91.67	0.82	4.78	14	
	Occipital Lobe	Lingual Gyrus	18	0.61	-85.62	-3.82	4.51	28	
	Occipital Lobe	Middle Occipital Gyrus	37	-38.23	-66.96	-0.91	3	19	
Visual Stimuli of 3D > 2D									
Right	Occipital Lobe	Lingual Gyrus	18	30.29	-70.69	-3.71	3.04	133	< .05
	Occipital Lobe	Lingual Gyrus	17	13.49	-89.94	1.39	2.99	133	
Left	Occipital Lobe	Lingual Gyrus	18	0.61	-85.62	-3.82	2.98	11	
	Occipital Lobe	Middle Occipital Gyrus	18	-29.09	-84.3	3.01	3.67	89	

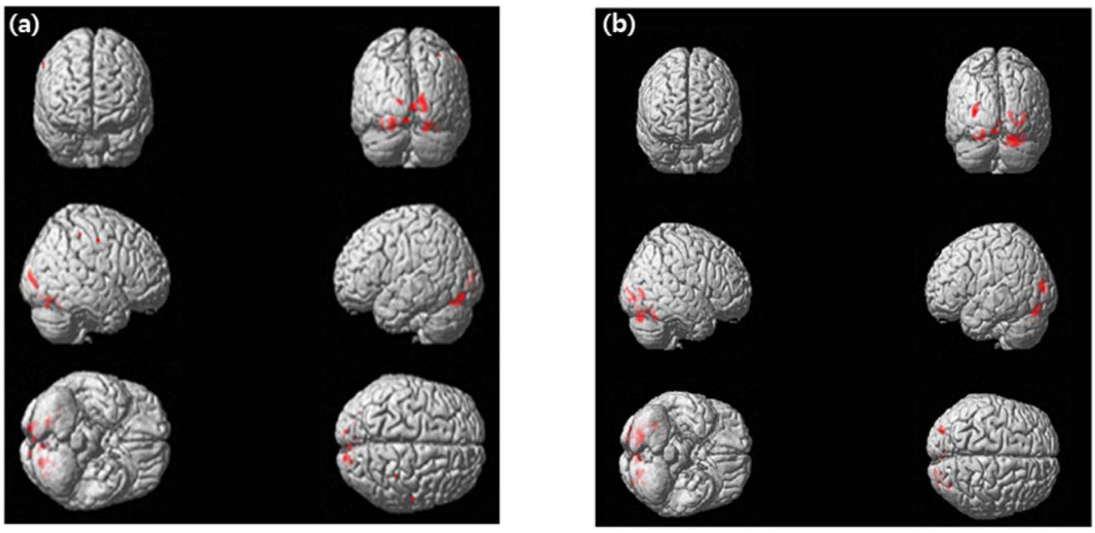

Fig. 4. (Color online) Results of Comparison between the Two-Dimensional (2D) and Three-Dimensional (3D) Stimulations: (a) region where the 2D image is stimulated more than the 3D image and (b) region where the 3D image is stimulated more than the 2D image.

the cerebral-cortex map was created by the German neurologist Korbinian Brodmann [8]. The BA cerebral-cortex map is divided into various areas including those of the somatosense, motor cortex, auditory sense, visual sense, and memory. In addition, it has been reported that the Talairach Daemon system that was used in this study can quickly access the Talairach atlas labs using the Talairach coordinates and can identify the BA labels with an accuracy of approximately 87 % [9]. The use of fMRI in neuroscientific research is a noninvasive means of identifying the active sites as the amount of oxygen in the blood stream increases [10, 11]. This is the BOLD tool, and it is the preferred scientific technique for the BA-based analysis of the active areas of the brain [12]. In this study, the difference between the activation degrees of the brain cortex were investigated using fMRI with the showing of 2D and 3D imagery. In the results of the 2D visual stimulation, the fusiform gyrus of the right occipital lobe, the lingual gyrus of the left occipital lobe, the precentral gyrus of the right frontal lobe, the parahippo-campal gyrus of the right limbic lobe, the postcentral gyrus of the right parietal lobe, the inferior parietal lobule, and the right temporal subgyral and middle temporal gyrus of the lobe showed a high activity. The effect of the

cortical stimuli varied according to the degree of the visual stimuli, but when the intensity of the visual stimuli was strong, it is linked to emotion-related organs such as the limbic system and the cingulate gyrus. According to Yeom *et al.* [13], an fMRI study of 50 highly intelligent Korean adults showed the activation of the prefrontal lobe to the vertebral cortex and the cerebral limbic system, including both the temporo-occipital cortex and the insula, when the visual stimulation was observed. This is consistent with the results of the visual stimulation of the 2D imagery in this study. In addition, Blondin *et al.* [14] showed photos of human-made objects and the natural scenes of 24 subjects and then performed fMRI activation studies according to the visual responses of the brain. In this report, the cerebral blood flow was increased in the last part of the visual processing when a photograph of a human-made object stimulated the parahippocampal gyrus, fusiform gyri, left occipital lobe, and temporal gyri. This means that the ability to perceive and recollect memory is increased when people see images that are familiar to them, demonstrating that the increases in the clusters from the parahippocampal gyrus and the fusiform gyrus are due to the stimulation of familiar objects such as triangular pyramids, cubes, and hexagonal columns with 2D images. That is, since the 2D-image stimulation experiment combined a picture that is familiar to the subject with a triangular pyramid, a cube, or a hexagonal column, it can be said that the visual stimulus works in combination with the memory region. Second, the 3D visual-stimulus results showed that the right occipital lobe of the lingual gyrus (BA 18), the middle occipital gyrus (BA 18), the superior frontal gyrus of the left frontal lobe (BA 6), the median frontal gyrus (BA 8), and the superior frontal gyrus (BA 8) showed a high activity. The BAs 6 and 8 are related to the working memory. Bledowski *et al.* [15] reported a working-memory analysis of 19 right-handed subjects for which fMRI was used and where the frontal gyrus is associated with attention. Langeben *et al.* [16] reported a false-positive response in the prefrontal-cortex area, which is the location of cognitive functioning, through the study of truth and false responses using fMRI. Greene *et al.* [17] also reported that damage to the median frontal gyrus plays an important role in decision-making as well as knowledge retention for members of normal society. In this study, it is very interesting that the 3D-image stimulation experiments showed strong reactions in the prefrontal cortex (BAs 6 and 8) that are involved in the working memory, as well as the visual cortex (BA 18). Based on the results of several studies, the subjects were only able to use the visual stimuli in the 2D imagery to produce a combined memory-area activity, which is the same as the other studies. However, when the 3D-image subjects were evaluated compared with the other studies, it is difficult to discern whether the prefrontal cortex was activated and to explain the reason for such activity. This difficulty is due to the existence of a number of possible interpretations, as follows: whether the 3D image enhanced the concentration of the subject [15], whether or not the subject recognized the fact that the imagery they were viewing is not reality [16], or whether the subject recognized that the imagery is not familiar knowledge (a 2D image that can be remembered). However, the results of the simple fMRI activation region show that the stimulations of the 2D and 3D images are clearly different in the human brain. In the present study, complaints such as the headache or vomiting were not expressed by the five subjects after the examination, so they were unable to participate in an examination of the occurrence of various diseases during or after the watching of 3D images. However, it is expected that 3D visualization will be a pioneering research area that scientifically proves that the watching of 2D images and other stimuli stimulates the human brain. In Japan, an episode of group neurological problems including the seizure and motion sickness was reported for a child who watched a *Pokemon* animation in December 1997 [18]. In this report, Furusho *et al.* [18] reported that the neurological problems occurred according to the viewing intensity, the distance between the screen and the eyes, and the surrounding brightness. The performance of a 3D-image analysis that is based on this report will also be necessary.

5. Conclusion

In this study, cerebral-activity differences were observed using fMRI according to the stimulations from 2D and 3D imagery. It was confirmed that the active area of the cerebrum changes according to the stimuli differences of the two images. This study is the first time that the activity of the human cerebrum during the viewing of 3D images has been scientifically demonstrated. In the future, it will be used as basic data in an analysis of the diffusion of 3D images and the corresponding social problems.

Acknowledgement

This work was supported in part by the Soonchunhyang university Research Fund.

References

[1] H. Y. Gao, Q. X. Yao, P. Liu, Z. Q. Zheng, J. C. Liu, H.

D. Zheng, C. Zeng, Y. J. Yu, T. Sun, and Z. X. Zeng, Chinese Phys. **25**, 9 (2016).
[2] Belton, J., An international journal. **24**, 2 (2012).
[3] B. Mark, R. Aire, S. Liis, Z. Nadezhda, Z. Olga, K. Anti, S. Bruno, and R. Aleksei, Front Neurol. **7**, 30 (2016).
[4] A.G. Solimini, A. M. Domitilla, D. D. Thience, and G. L. Torre, BMC Public Health. **12**, 1 (2012).
[5] J. C. Read and I. Bohr, Ergonomics. **57**, 8 (2014).
[6] M. Taylor, A. Anish, and C. Bush, Clin Cardiol. **34**, 11 (2011).
[7] U. Kâmil, J. D. David, and B. B. Richard, Basic Principles of functional MRI (Clinical MRI, San Diego, 2005), Vol. 1, Chap. 9, pp. 249-287.
[8] M. Louksa, P. Christopher, G. Christopher, T. R. Shane, PA-C, and A. A. Cohen-Gadol, Neurosurgery **68**, 1 (2011).
[9] L. L. Jack, G. W. L. M. P. M. L. Marty, S. F. L. R. Catarina, V. K. D. N. Peter, and A. M. P. T. F. Shawn, Hum Brain Mapp. **10**, 3 (2000).
[10] C. H. Friedhelm and G. C. Leonardo, Neurology. **5**, 8 (2006).
[11] A. Grinvald, H. Solvin, and I. Vanzetta, Nat Neurosci. **3**, 2 (2000).
[12] J. A. Owen and B. Simon, Trends Neurosci. **25**, 1 (2002).
[13] S. M. Yeom, S. H. Jeon, M. K. Yi, D. E. Kim, and D. W. Yang, KJ-HSM. **7**, 101 (2013).
[14] F. Blondin and M. Lepage, Neuropsychologia. **43**, 13 (2005).
[15] C. Bledowski, B. Rahm, and J. B. Rowe, J Neurosci. 29, 43 (2009).
[16] D. D. Langleben, J. W. Loughead, W. B. Biker, K. Ruparel, A. R. Childress, S. I. Busch, and R. C. Gur, Hum Brain Mapp. **26**, 4 (2005).
[17] J. Greene and J. Haidt, Trends Cogn Sci. **6**, 12 (2002).
[18] J. Furucho, M. Suzuki, I. Tazaki, H. Satoh, K. Yamaguchi, Y. Likura, K. Kumagai, T. Kubagawa, and T. Hara, Pediatr Neurol. **27**, 5 (2002).